

On the use of motion-based frame rejection in temporal averaging denoising for segmentation of echocardiographic image sequences

Maria do Carmo dos Reis, João L. A. Carvalho, Bruno L. Macchiavello, Daniel F. Vasconcelos, Adson F. da Rocha, Francisco A. O. Nascimento, and Juliana F. Camapum

Abstract—We have recently introduced an algorithm for semi-automatic segmentation of the left ventricular wall in short-axis echocardiographic images (EMBC 30:218–221). In its preprocessing stage, the algorithm uses temporal averaging for image denoising. Motion estimation is used to detect and reject frames that do not correlate well with the set of images being averaged. However, the process of estimating motion vectors is computationally intense, which increases the algorithm’s computation time. In this work, we evaluate the viability of replacing the motion estimation stage with less computationally intense approaches. Two alternative techniques are evaluated. The ventricular contours obtained from each of the three algorithm variants were quantitatively and qualitatively compared with contours manually-segmented by a specialist. We show that it is possible to reduce the algorithm’s computational load without significantly reducing the segmentation quality. The proposed algorithms are also compared with three other techniques from the literature.

Keywords: segmentation, echocardiographic images, motion estimation, area variation, boundary detection.

I. INTRODUCTION

Echocardiography is the current non-invasive gold standard for real-time assessment of cardiac function. The segmentation of ventricular walls in echocardiographic images is used for measuring ventricular volume, which is important in evaluating many cardiovascular conditions [1].

Several algorithms for ventricular wall segmentation have been proposed in the literature. These include algorithms designed for short-axis [2]–[4] and long-axis images [5], [6], semi-automatic algorithms [1], [3], and fully-automated algorithms [6]–[8]. In the preprocessing stage, several different approaches have been used for denoising, such as morphologic filtering [1], the discrete wavelet transform [7], and temporal averaging [9].

We have recently introduced an algorithm for semi-automatic segmentation of left ventricular (LV) wall in sequences of short-axis echocardiographic images [10]. The preprocessing stage consists of (i) temporal averaging denoising, (ii) contrast enhancement, using a self-reinforced edge-enhancement hi-pass filter and a Laplacian of Gaussian (LoG) filter, and (iii) morphological closing. The

segmentation stage consists of histogram-based thresholding, region labeling, and neighborhood operations. The latter is used to detect the LV boundary pixels. In the temporal averaging step, this algorithm uses motion estimation to detect and reject frames that do not correlate well with the set of images being averaged. However, the process of estimating motion vectors is computationally intense, which increases the algorithm’s computation time.

In this work, we evaluate the viability of replacing the motion estimation stage with less computationally intense approaches. Two alternative techniques are evaluated. In the first approach, motion detection is performed by taking the pixel-by-pixel difference between frames. In the second approach, motion detection and frame rejection are not performed, but a smaller temporal window is used for averaging. The ventricular contours obtained from each of these three algorithm variants were quantitatively and qualitatively compared with contours manually-segmented by a specialist. The computation times are also evaluated. Finally, the proposed algorithms are compared with three other approaches from the literature.

II. METHODS

A. Image segmentation algorithm

The proposed algorithm for segmentation of echocardiographic image sequences is designed in two stages, and six substages:

1. Preprocessing
 - a. temporal averaging denoising
 - b. contrast enhancement
 - c. morphological closing
2. Segmentation
 - a. histogram-based thresholding
 - b. region labeling
 - c. neighborhood operation.

In our original implementation [10], temporal averaging denoising is implemented as follows. A set of ten consecutive images are used to produce a temporally-averaged image. A sliding-window approach is used to produce one averaged image for each new image in the sequence, i.e., the sliding window step is one (Fig. 1). For each window, the optic flow matrix (motion vectors) between adjacent frames is calculated for the set of ten images (Fig. 2). The motion estimation process consists in segmenting the image in macroblocks (16×16 in this work), and then searching, within a region-of-interest of the

Manuscript received April 7, 2009.

M. C. dos Reis, J. L. A. Carvalho, B. L. Macchiavello, A. F. da Rocha, F. A. O. Nascimento and J. F. Camapum are with the Electrical Engineering Department, University of Brasília, Brasília, DF, Brazil (e-mail: juliana@ene.unb.br).

D. F. Vasconcelos is with the Medicine Faculty and the Electrical Engineering Department, University of Brasília, Brasília, DF, Brazil.

reference image, the best correlated block of pixels of the same size. In our implementation, diamond search was used. Then, the total motion is quantified by taking the sum of all motion vector magnitudes in the optic flow matrix. The five frames with stronger motion are removed from the image set, and the remaining five images are averaged (pixel-by-pixel), producing a denoised image. These numbers were empirically chosen.

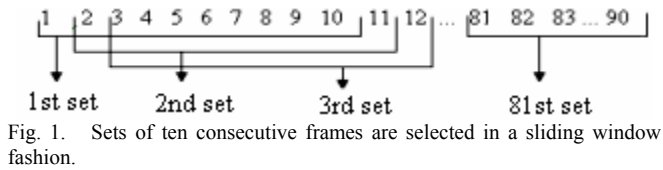


Fig. 1. Sets of ten consecutive frames are selected in a sliding window fashion.

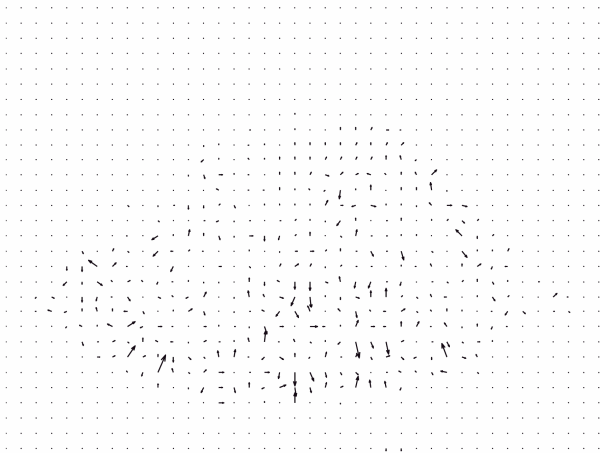


Fig. 2. Optic flow measured from two consecutive frames.

The next step of preprocessing is contrast enhancement, using a self-reinforced edge-enhancement hi-pass filter, and a LoG filter. Then, morphological closing is used to obtain a uniform LV cavity. In the segmentation stage, the LV boundary pixels are detected using three processes, in sequence: (i) histogram-based thresholding, (ii) region labeling, and (iii) neighborhood operations. The left ventricular area is calculated by counting the number of pixels within the segmented contour and multiplying this by the pixel area. The LV area is calculated for each image in the sequence, i.e., for each sliding window position. The area variation curve associated with a complete cardiac cycle is constructed by interpolating the measured areas, using 10th-order polynomial fit (see Fig. 7, discussed later). A more detailed description of this algorithm is presented in ref. [10].

B. Motion quantification using image subtraction

In the temporal averaging denoising stage (step 1a) of the segmentation algorithm discussed above, the calculation of the degree of motion between images may be more simply performed by calculating the absolute mean of the pixel-by-

pixel difference between two adjacent frames (i.e., image subtraction). This process is significantly less computationally intense than calculating the optic flow matrix, as originally proposed. However, it may also be less precise, especially in the presence of noise.

In this alternate implementation of the algorithm, the same 10-frame step-1 sliding window approach is used (Fig. 1). For each sliding window position, the pixel-by-pixel difference between each pair of adjacent images is calculated (Fig. 3). Then, the absolute sum of all pixels in the difference image is calculated. This is used as an estimate of the degree of motion between the two images. The five frames with stronger motion are removed from the image set, and the remaining five images are averaged (pixel-by-pixel), producing a denoised image. The subsequent preprocessing and segmentation steps are performed exactly as described in the previous section.

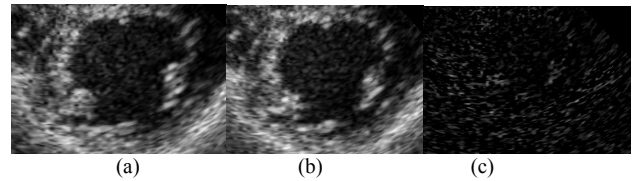


Fig. 3. A pair of temporally-adjacent frames (a,b), and the pixel-by-pixel difference between the two (c).

C. Temporal averaging without frame rejection

Alternatively, temporal averaging denoising may be performed without frame rejection, thus eliminating the need for motion quantification. However, in this case it is necessary to use a smaller sliding window size.

In this implementation of the algorithm, a 5-frame step-1 sliding window approach was used (Fig. 4). All five temporal frames in the window are averaged (pixel-by-pixel), producing a denoised image. The subsequent preprocessing and segmentation steps are performed exactly as described in section II.A.

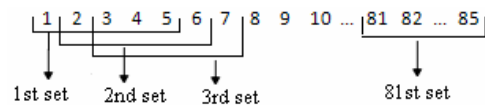


Fig.4. Sliding window approach for temporal averaging denoising, using a smaller window size.

D. Performance evaluation

A set of 25 short-axis echocardiographic images from 13 patients was used to evaluate the performance of the proposed algorithms. Images were acquired on a Philips ATL HDI-3500 system. A cardiologist, specialist in the field of echocardiography, manually segmented the LV wall boundary in each image, and classified the images in three groups: good quality (10 images), average quality (10 images), and poor quality (5 images). This classification was based on image contrast and boundary definition.

The LV contours obtained with each method were quantitatively compared with the manually-segmented contours, using four metrics: cross-correlation coefficient (CCC), percent error (PE) [11], error sum (ES) [11], and edge-positioning error (EPE) [12]. Let M and A be $m \times n$ binary images, associated with the manually segmented and semi-automatically segmented contours, respectively, in which pixels within the contour (inclusive) are set to 1, and all other pixels are set to 0. Then, CCC is a measurement of similarity between images M and A , PE is a measurement of the area estimation error, and ES and EPE are measurements of the edge-positioning error, as follows:

$$CCC = \frac{|\tilde{A} \cdot \tilde{M}|}{\sqrt{|\tilde{A} \cdot \tilde{A}| \cdot |\tilde{M} \cdot \tilde{M}|}} \quad (1)$$

$$PE = \frac{|M| - |A|}{|M|} \times 100\% \quad (2)$$

$$ES = \frac{|M \cap \tilde{A}| + |\tilde{M} \cap A|}{|M|} \times 100\% \quad (3)$$

$$EPE = \frac{|M \cap \tilde{A}| + |\tilde{M} \cap A|}{\rho} \quad (4)$$

where $|X|$ is the sum of all pixels in image X , $\tilde{X} = X - x$, where x is the mean value of image X , i.e., $x = |X| / (m \cdot n)$, $X \cdot Y$ denotes pixel-by-pixel image multiplication, \tilde{X} is the complement of image X (binary pixel inversion), ρ is the perimeter of the manually-segmented contour (in pixels), and \cap denotes intersection.

The algorithms were implemented on Matlab 6.5 (The MathWorks, Inc., Natick, MA, USA), and the processing time for each algorithm variant was measured for a sequence of 90 images (81 contours) on a personal computer with an Intel Pentium 4 processor with 3.2GHz clock and 1GB of RAM, running Microsoft Windows XP.

III. RESULTS AND DISCUSSION

Figures 5 and 6 show contours obtained with each algorithm variant and their superposition with the manually-segmented contours, for representative images classified as of good and medium qualities, respectively. All three semi-automatic approaches presented good agreement with the manually-segmented contours, especially for good quality images. The results achieved by the proposed methods were considered accurate by two echocardiography specialists.

Figure 7 presents the area variation curve calculated for a representative healthy volunteer, over a complete cardiac cycle, using each algorithm variant. This curve provides additional information to the cardiologist or specialist about the subject's ventricular function [10]. The algorithms based on motion quantification produce better results than the small sliding window approach. Fewer false negatives (area = 0) are observed, and the curves present fewer abrupt discontinuities and overestimation/underestimation artifacts, resulting in a smoother waveform. Such variations do not represent physiological behavior and are considered artifacts. Nevertheless, the results obtained with the small

sliding window approach show reasonable agreement with the other two methods, and the observed small reduction in accuracy may be compensated by the significant reduction in processing time and complexity.

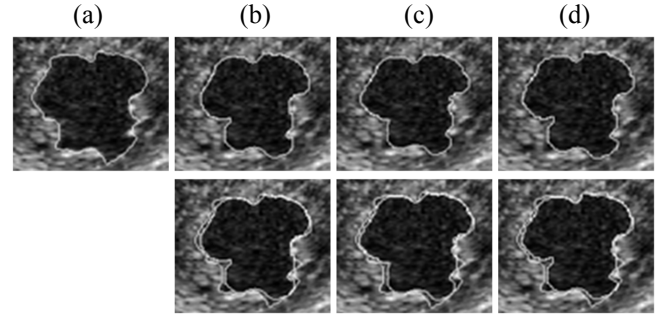


Fig. 5. Left ventricular wall contours for good quality images: (a) manually-segmented; (b) optic flow method; (c) image subtraction method; (d) small sliding window method. Bottom row presents a superposition over the manually-segmented contour.

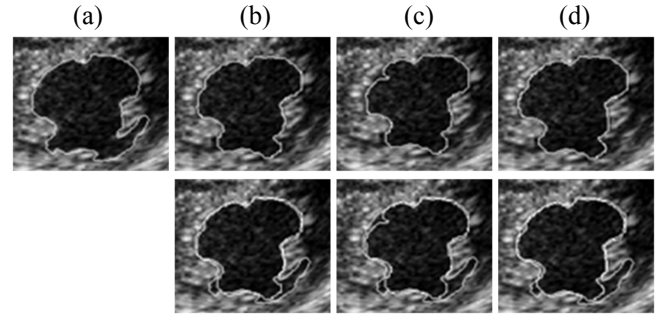


Fig. 6. Left ventricular wall contours for medium quality images: (a) manually-segmented; (b) optic flow method; (c) image subtraction method; (d) small sliding window method. Bottom row presents a superposition over the manually-segmented contour.

The results from the quantitative comparison are presented in Table 1. The results show that the proposed methods are capable of providing LV-wall contour estimates with a high degree of accuracy, especially for good and medium quality images. The results for the low quality images were not completely satisfactory, but this is an expected result, since the manual segmentation of low quality echocardiography images is also commonly inaccurate. The results obtained with the small sliding window approach were equivalent to those obtained with the approach based on image subtraction, but at a considerably lower computational load. These two approaches resulted in slightly higher error levels than the method based on optic flow calculation, but achieved a significant reduction in processing time.

Results from literature (refs. [3], [7] and [12]) are also presented in Table 1, for comparison. For good quality images, the method based on optic flow calculation achieves mean errors equivalent to those reported by de Andrade *et al.* [7]. However, the proposed methods presented lower PE and ES standard deviation, which implies better consistency. For good quality images, the proposed methods achieved equivalent or better cross-correlation with manual-segmentation than those reported by Klingler *et al.* [3],

Table 1 – Quantitative comparison between the three proposed approaches and other methods from the literature.

	<i>image quality - # of images</i>	<i>CCC^a</i>	<i>PE (%)^b</i>	<i>ES (%)^b</i>	<i>EPE^c</i>	<i>Proc. Time^d</i>
Optic flow [10]	good - 10	0.95	3.52 ± 1.24	9.47 ± 2.02	1.04<EPE<1.21	20 min
	medium - 10	0.90	11.96 ± 3.38	16.49 ± 2.15	2.01<EPE<2.61	
	low - 5	0.68	21.98 ± 7.04	35.50 ± 7.27	5.04<EPE<5.95	
Pixel-by-pixel subtraction	good - 10	0.94	6.15 ± 2.56	11.38 ± 3.05	1.14<EPE<1.41	10 min
	medium - 10	0.90	12.71 ± 4.36	13.32 ± 3.99	2.61<EPE<2.91	
	low - 5	0.67	23.65 ± 8.36	36.32 ± 8.32	5.91<EPE<6.95	
Small sliding window	good - 10	0.93	6.40 ± 2.60	11.98 ± 3.19	1.25<EPE<1.52	6 min
	medium - 10	0.88	14.36 ± 3.95	14.01 ± 4.02	2.97<EPE<3.99	
	low - 5	0.63	24.99 ± 8.55	36.02 ± 9.08	6.08<EPE<7.11	
de Andrade <i>et al.</i> [7]	good - 20	0.98	2.49 ± 2.46	9,62 ± 7,9	-	-
Klingler <i>et al.</i> [3]	-	0.93	-	-	-	-
Coppini <i>et al.</i> [12]	500	-	-	-	0.53<EPE<0.77	-

^a mean value; ^b mean ± standard deviation; ^c dynamic range; ^d processing time for a sequence of 90 images (81 contours).

however their work does not specifies image quality conditions. The proposed methods achieved larger edge-positioning errors than those reported by Coppini *et al.* [12], however their work focused on apical images rather than short-axis images.

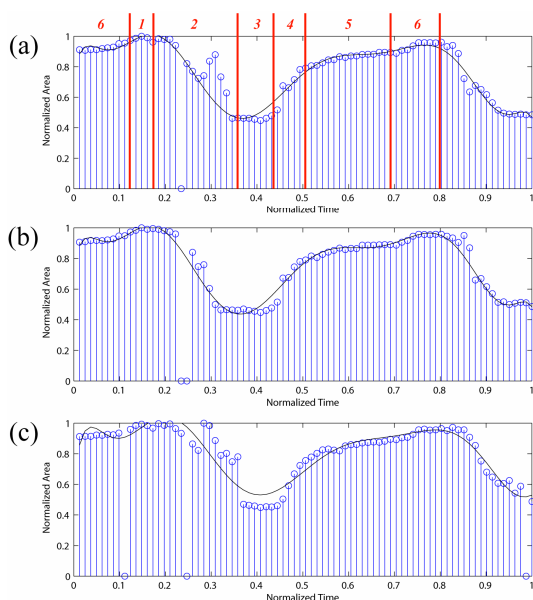


Fig. 7. Area variation curve for a representative subject, measured with each algorithm: (a) optic flow; (b) pixel-by-pixel subtraction; (c) small sliding window. Blue circles indicate measured areas, and solid black lines represent the interpolated curves. The phases of the cardiac cycle are indicated: (1) isovolumetric contraction; (2) ejection; (3) isovolumetric relaxation; (4) rapid filling; (5) reduced filling; (6) atrial systole.

IV. CONCLUSIONS

We have proposed and demonstrated an algorithm for accurate semi-automatic segmentation of left ventricular wall in short-axis echocardiographic images. Three different approaches to frame-selection in temporal averaging denoising were qualitatively and quantitatively evaluated. The results show that it is possible to eliminate the computationally-intense process of calculating the optic flow matrix by using a smaller sliding window for temporal averaging, at the expense of a small reduction in segmentation precision. The results were also shown to be equivalent or more accurate than other methods from the

literature. The proposed algorithm may facilitate the diagnosis of various cardiac conditions that affect left ventricular function.

REFERENCES

- [1] M. M. Choy, and S. J. Jesse, "Morphological image analysis of left-ventricular endocardial borders in 2D echocardiograms," *SPIE Proc. on Medical Imaging*, vol. 2710, pp. 852–863, 1996.
- [2] V. Chalana, D. T. Linker, D. R. Haynor, and Yongmin Kim, "A multiple active contour model for cardiac boundary detection on echocardiographic sequences," *IEEE Trans. on Medical Imaging*, vol. 15, n. 3, pp. 290–298, 1996.
- [3] J. W. Klingler Jr., C. L. Vaughan, T. D. Fraker Jr., and L. T. Andrews, "Segmentation of echocardiographic images using mathematical morphology," *IEEE Trans. on Biomedical Engineering*, vol. 35, n. 11, pp. 925–934, Nov. 1988.
- [4] A. Laine, and X. Zong, "Border Identification of Echocardiograms via multiscale edge detection and shape modeling," in *Proc. of the IEEE Int. Conf. on Image Processing*, vol. 3, pp. 287–290 vol.3, Sep. 1996.
- [5] Jierong Cheng, Say Wei Foo, and Shankar M. Krishnan, "Automatic Detection of Region of Interest and Center Point of Left Ventricle using Watershed Segmentation," in *Proc. IEEE Int. Symposium on Circuits and Systems*, vol. 1, n. 2, pp. 149–151, May 2005.
- [6] Jierong Cheng, Say Wei Foo, and Shankar M. Krishnan, "Watershed-Presegmented Snake for Boundary Detection and Tracking of Left Ventricle in Echocardiographic Images," *IEEE Trans. on Information Technology in Biomedicine*, vol. 10, n. 2, pp. 414–416, 2006.
- [7] M. M. de Andrade, B. L. Macchiavello, F. A. de O. Nascimento, A. F. da Rocha, H. S. Carvalho, and P. C. Jesus, "Algoritmo híbrido para segmentação do ventrículo esquerdo em imagens de ecocardiografia bidimensional," *Revista Brasileira de Engenharia Biomédica*, vol. 22, pp. 30–39, 2006.
- [8] I. Koren, A. F. Laine, J. Fan, and F. J. Taylor, "Edge detection in echocardiographic image sequences by 3-D multiscale analysis," in *Proc. IEEE Int. Conf. on Image Processing*, vol. 1, pp. 288–292, 1994.
- [9] B. L. Macchiavello, M. M. de Andrade, F. A. de O. Nascimento, H. S. Carvalho, D. F. Vasconcelos, A. F. da Rocha, and S. A. de Melo Jr., "Algoritmo de segmentação de eco 2D dinâmica," in *Proc. XXVIII CILAMCE/CMNE (Congresso de Métodos Numéricos em Engenharia)*, Porto, Portugal, vol. 1, pp. 1–16, 2007.
- [10] M. C. dos Reis, A. F. da Rocha, D. F. Vasconcelos, B. L. M. Espinoza, F.A.O. Nascimento, J.L.A. Carvalho, and J. F. Camapum, "Semi-automatic detection of the left ventricular border," in *Proc. 30th International Conference, IEEE Engineering in Medicine and Biology Society*, 2008, Vancouver, pp. 218–221, 2008.
- [11] P. Lilly, J. Jenkins, and P. Bourdillon, "Automatic Contour Definition on Left Ventriculograms by Image Evidence and a Multiple Template-Based Model," *IEEE Trans. on Medical Imaging*, vol. 8, n. 2, pp. 173–185, 1989.
- [12] G. Coppini, R. Poli, and G. Valli, "Recovery of the 3-D Shape of the Left Ventricle from Echocardiographic Images," *IEEE Transactions on Medical Imaging*, vol. 14, n. 2, pp. 301–317, 1995.